A Data-Driven Hybrid Model Predictive Control Framework for Managing Epidemics Using 3DoF-KF HMPC

Sarasij Banerjee[1], Mohamed El Mistiri[1], Owais Khan[1], and Daniel E. Rivera[1]

***Abstract*— This paper describes a systematic approach for epidemic control using control-relevant identification coupled with a multi-input, multi-output 3-Degree-of-Freedom Kalman filter-based Hybrid Model Predictive Control (MIMO 3DoF-KF HMPC) featuring online controller reconfiguration. The combined data-driven modeling and control strategy is evaluated on a Susceptible-Infected-Recovered (SIR) model involving vaccination and loss of immunity (i.e., reinfection). "Zippered" multisine input signals and ARX estimation are applied to obtain a multivariable dynamic model that is the basis for an HMPC algorithm featuring both continuous and categorical (i.e., discrete level) actions through a Mixed Integer Quadratic Programming (MIQP) formulation. The goal is to reduce the infected population while balancing societal impacts. The hybrid formulation with reconfiguration dynamically adjusts health intervention policies, such as categorical lockdown levels and continuous vaccination rates. This approach enables operational goals such as reducing the infected population to a desired interval or relaxing lockdown to a designated setpoint; furthermore, the 3DoF formulation enables independent tuning for setpoint tracking and measured and unmeasured disturbance rejection, allowing scalable solutions across diverse epidemiological settings. The framework is demonstrated through two demanding case studies involving 90% infection reduction under time-varying recovery and loss of immunity. The resulting closed-loop model provides a practical tool for guiding government policy and public decisions during pandemics.**

I. Introduction

The COVID-19 pandemic has emphasized the necessity for practical and effective strategies to limit the spread of infectious diseases. Public health interventions such as lockdowns, masking, and vaccination are essential but require careful balancing of health and societal impacts. Dynamic modeling and control of infectious disease processes such as the *Susceptible-Infected-Recovered* (SIR) [1], [2] model featuring physical contact, transmission, loss of immunity, vaccination, and recovery, have garnered significant attention for effectively implementing well-established laws of control systems engineering to devise efficient algorithms to cope with various disease-spread scenarios. However, determining optimal interventions remains a challenge, especially when real-world policies like lockdowns are inherently categorical, unlike continuous control strategies traditionally used in epidemiological models [3], [4].

This paper develops a proof-of-concept epidemic control strategy using a multi-input, multi-output 3-Degree-of-Freedom Kalman filter-based Hybrid Model Predictive Control (MIMO 3DoF-KF HMPC) [5], incorporating continuous and discrete control actions through Mixed Logic Dynamic (MLD)-based predictive modeling. Social distancing policies such as lockdowns are treated as categorical variables that allow for a rapid, large-scale reduction in infection over the short term, while continuous vaccination enables incremental adjustments to balance health and societal needs. This facilitates long-term reduction in the infected population and simultaneous relaxation of social distancing requirements, prompting a return to normalcy.

This MIMO formulation in a 3DoF setting allows independent tuning parameters for setpoint tracking and measured and unmeasured disturbance rejection, which is very akin to IMC tuning [6], making it more intuitive than conventional move-suppression and weight-based MPC for simultaneously addressing different performance objectives such as infection reduction or adjustment of lockdown and vaccination in response to recovery or reinfection.

It is important to note that the control performance of the 3DoF-KF HMPC greatly depends on the prediction ability of its dynamic model. Incorporating simple AutoRegressive with eXogenous inputs (ARX)-based data-centric models [7] into the HMPC framework, in particular, offers significant advantages in terms of flexibility and adaptability to nonlinearities while maintaining the accessibility of linear techniques. ARX modeling is enabled through the use of systematically designed multisine signals that are implemented on the nonlinear SIR model in a plant-friendly manner. The 3DoF-KF ARX HMPC, therefore, provides a robust tool for decision-makers to optimize public health interventions in the presence of abundant epidemiological data.

The framework is tested in simulated settings using two case studies. These include manipulating different MPC objective weights to attain control configurations with varied interests. The standard case explores the benefits and challenges of the MIMO hybrid formulation, while the second case study introduces a reconfiguration policy that emphasizes the sensible use of resources and explains the need to balance control efforts with infection reduction objectives.

The paper is structured as follows: Section II introduces a first-principles description of the SIR model that serves as the basis for data-driven modeling of infection dynamics. Section III provides detailed descriptions pertaining to the experiment design, ARX-based data-centric modeling, and the formulation of the HMPC framework, including the logical constraints, the 3DoF formulation, and the resulting MIQP. Section IV describes the case studies involved in validating the framework. Section V concludes the paper with a summary and direction for future work.

[1]S. Banerjee, M. El Mistiri, O. Khan, and D. E. Rivera are with the Control Systems Engineering Laboratory, School for Engineering of Matter, Transport, and Energy, Arizona State University, Tempe, AZ 85287 USA.

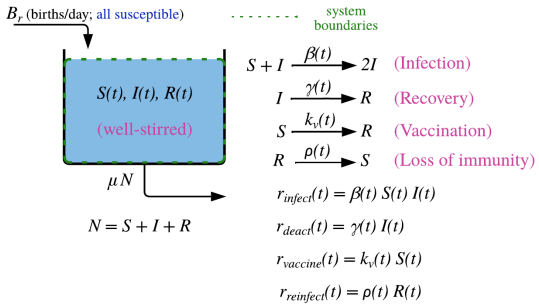

Fig. 1: SIR model illustrated as a continuous stirred tank reactor system, demonstrating autocatalytic (infection) and deactivation (recovery) reactions, along with vaccination and loss of immunity.

II. SIR Model for Disease Transmission

The SIR model considered in this work is a parsimonious system of differential equations inspired by a Continuous Stirred Tank Reactor (CSTR) analogy [2], as depicted in Figure 1. It models the spread of infectious disease across three compartments of the population: - *Susceptible* (*S(t)*), *Infected* (*I(t)*), and *Recovered* (*R(t)*). The transition from $S(t)$ to $I(t)$ mimics an irreversible autocatalytic chemical reaction and occurs at the infection rate $\beta(t)$ as:

$$S + I \overset{\beta(t)}{\rightarrow} 2I \qquad r_{infect}(t) = \beta(t)S(t)I(t) \tag{1}$$

where $r_{infect}(t)$ denotes the rate of the reaction. The transfer of population from $I(t)$ to $R(t)$ is characterized by a first-order irreversible reaction given by:

$$I \overset{\gamma(t)}{\rightarrow} R \qquad r_{deact} = \gamma(t)I(t) \tag{2}$$

where $\gamma(t)$ denotes the daily recovery rate and r_{deact} refers to the corresponding rate of reaction. Vaccination ($k_v(t)$) directly transfers individuals from $S(t)$ to $R(t)$:

$$S(t) \overset{k_v(t)}{\rightarrow} R(t) \qquad r_{vacc} = k_v(t)S(t) \tag{3}$$

Loss of immunity ($\rho(t)$) returns a certain portion of the recovered population to the susceptible class as:

$$R(t) \overset{\rho(t)}{\rightarrow} S(t) \qquad r_{reinfect}(t) = \rho(t)R(t) \tag{4}$$

with reaction rate $r_{reinfect}(t)$.

Daily birth rate B_r adds to $S(t)$, while a daily mortality rate μ removes the population from all three compartments. For the sake of simplicity, B_r and μ are considered constants throughout the study, and it is assumed that μ remains equal across all three compartments ($\mu = \mu_S = \mu_I = \mu_R$). The total population is considered to be constant ($N = S(t)+I(t)+R(t)$), with $R(t)$ being evaluated from $S(t)$ and $I(t)$ at any given point. This system of disease transmission dynamics can be represented as:

$$\begin{aligned}\frac{dS(t)}{dt} = &\underbrace{B_r}_{\substack{Births\\(inflow)}} - \underbrace{\beta(t)S(t)I(t)}_{\substack{Infection\\(consumption)}} - \underbrace{\mu S(t)}_{\substack{Mortality\\(outflow)}} \\ &- \underbrace{k_v(t)S(t)}_{\substack{Vaccination\\(consumption)}} + \underbrace{\rho(t)\left(\frac{B_r}{\mu} - S(t) - I(t)\right)}_{\substack{Loss\ of\ Immunity/Reinfection\\(generation)}}\end{aligned} \tag{5}$$

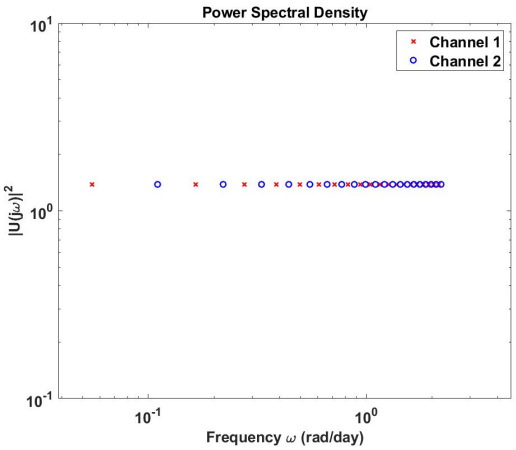

Fig. 2: Power spectra for zippered input design: $\beta(t)$ (Channel 1) and $k_v(t)$ (Channel 2), generated using minimum Crest Factor multisine signals [8].

$$\frac{dI(t)}{dt} = \underbrace{\beta(t)S(t)I(t)}_{\substack{Infection\\(consumption)}} - \underbrace{\gamma(t)I(t)}_{\substack{Deactivation\\(consumption)}} - \underbrace{\mu I(t)}_{\substack{Mortality\\(outflow)}} \tag{6}$$

Setting the differential equations (5)-(6) characterizing the SIR model to zero leads to endemic steady state conditions $\{\overline{S}, \overline{I}, \overline{R}\}$ with a non-zero infected population at the start of the study [3]. This framework enables a control systems approach, treating $I(t)$ as the output of interest, $\beta(t)$, $k_v(t)$ as the manipulated variables, $\gamma(t)$ as the measured disturbance, and $\rho(t)$ as an unmeasured disturbance. To develop measures that are more socially sustainable, and recognizing the flexibility of treating $k_v(t)$ as a second manipulated variable, a target is also set for $\beta(t)$. This helps to relax lockdown policies while keeping the infection rate within the desired range, making $\beta(t)$ another key output to monitor.

III. Data-Driven Modeling and Control for Epidemiology Intervention

The nonlinear dynamics of the SIR model vary considerably depending on the operating points, making it crucial to develop a database that spans all regions of infection dynamics for effective modeling of the disease transmission. The database for this problem was obtained by a systematic design of plant-friendly input signals, which, when introduced into the SIR model characterized by equations (5) and (6), generated sufficient excitation for capturing the dynamics using data-centric modeling.

A. Experiment Design and Model Estimation

The input signals associated with the two manipulated variables $\beta(t)$ and $k_v(t)$ were designed with zippered multisine signals [9] involving two channels that are orthogonal in the frequency domain, given by:

$$\begin{aligned} u_n(k) &= \lambda_n \sum_{i=1}^{n_s} \sqrt{2\alpha_{n,i}}\, cos(\omega_i k T_s + \phi_{[n,i]}) \\ \omega_i &= \frac{2\pi i}{N_s T_s}, \quad k = 1, \cdots, N_s \end{aligned} \tag{7}$$

where λ_n represents the scaling factor, N_s denotes the number of samples per period of the signal, and T_s is the

TABLE I: Nominal parameters for plant dynamics of the SIR model. $\overline{*}$ - Steady-state value.

Parameters	Units	Values	Parameters	Units	Values
B_r	Persons/Day	500	$\overline{\beta}$	Person^{-1}Day^{-1}	0.001
μ	Day^{-1}	0.08	$\overline{\gamma}$	Day^{-1}	0.35
$\overline{k}_v$	Day^{-1}	0	$\overline{\rho}$	Day^{-1}	0.05
$\overline{S}$	Persons	1100	$\overline{I}$	Persons	2966
$\overline{R}$	Persons	5934	N	Persons	10000

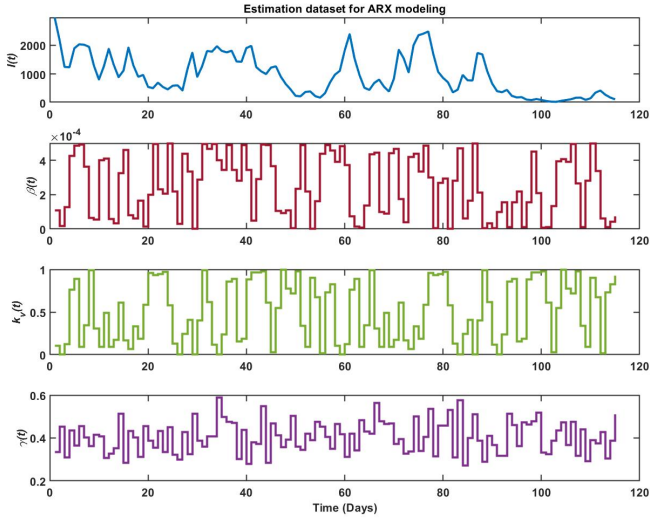

Fig. 3: Estimation dataset featuring zippered $\beta(t)$ and $k_v(t)$ signals, white-noise-based $\gamma(t)$, and resultant $I(t)$. Validation datasets use different signal realizations with $\rho(t)$ fixed at $\overline{\rho} = 0.05$.

sampling time. $n_s \leq N_s/2$ denotes the number of sinusoids. For the *i*-th harmonic of the signal, $\alpha[n,i]$ specifies the relative power of the harmonic, ω_i represents the frequency, and $\phi_{[n,i]}$ is the phase. For $n = n_u$ channels, zippering is obtained by specifying the relative powers as follows:

$$\alpha[n,j] = \begin{cases} 1 & \text{if } j = n_u(i-1)+n \quad \text{for } i = 1,2,\ldots,n_s \\ 0 & \text{otherwise} \end{cases} \tag{8}$$

The main frequency band of interest for these signals lies in the interval $[\omega_*, \omega^*]$, given by:

$$\omega_* = \frac{1}{\beta_s \tau_{dom}^H} \leq \omega \leq \frac{\alpha_s}{\tau_{dom}^L} = \omega^* \tag{9}$$

where $\tau_{dom}^H, \tau_{dom}^L$ denote the estimated high and low values of the dominant time constants of the model respectively, and α_s and β_s denote parameters associated with the high and low-frequency ranges of interest.

Based on the step test of the SIR model, the time constants were chosen to be τ_{dom}^H = 3 days and τ_{dom}^L = 1 day. The multipliers for choosing suitable bandwidth included setting α_s = 2, β_s = 3, resulting in the power spectrum in Figure 2.

The phases were determined using a minimum crest-factor approach [8] to ensure plant-friendliness. Signal amplitudes for the SIR problem were designed using *a priori* system knowledge: $\overline{\beta}$ = 0.8 Persons/Day for $\beta(t)$, 1 Day^{-1} for $k_v(t)$, and band-limited white noise with power 0.005 for $\gamma(t)$. Different realizations of input signals with the same frequency content were used to create estimation and validation datasets (Figure 3). Infection dynamics were modeled using parsimonious ARX models [7] with a regressor structure $[n_a \quad n_{b_j} \quad n_{k_j}]_{j=1,\cdots,n_u}$. A [2 [2 2 2] [1 1 1]] structure achieved an NRMSE fit of 47.6% on validation data (Figure 4) and 57.2% on the estimation dataset, with the resulting model being readily integrated into the 3DoF-KF HMPC framework via state-space formulation [5].

Higher-order models such as an ARX with [4 [4 4 4] [1 1 1]] with NRMSE fit of 53% on validation data and a [2 [2 2 2] [1 1 1]] based Model-on-Demand [10] estimator with NRMSE fit of 56% on validation data were also tested in generating models. While these models clearly demonstrated benefits in open-loop settings, their closed-loop performance (not included for brevity) did not showcase noticeable improvements, thereby resulting in the choice of the [2 [2 2 2] [1 1 1]] ARX model for the control results in this paper.

B. Controller Formulation

The hybrid control-oriented approach to epidemic management aims to achieve a desired infection target by optimizing distancing and vaccination decisions while considering societal constraints, such as:

- Maximum and minimum imposable lockdown and vaccination policies.
- Lockdown levels chosen from predefined discrete values to ensure practical implementation.
- Multi-stage interventions with varying priorities, such as minimizing infections or relaxing measures once target infection rates are met.

A solution can be obtained through the formulation of the SIR problem as a mixed logic dynamic (MLD) followed by the implementation of a hybrid MPC framework. This approach restricts social distancing to transparent, predefined levels, improving societal acceptance. The following subsections present the detailed formulation:

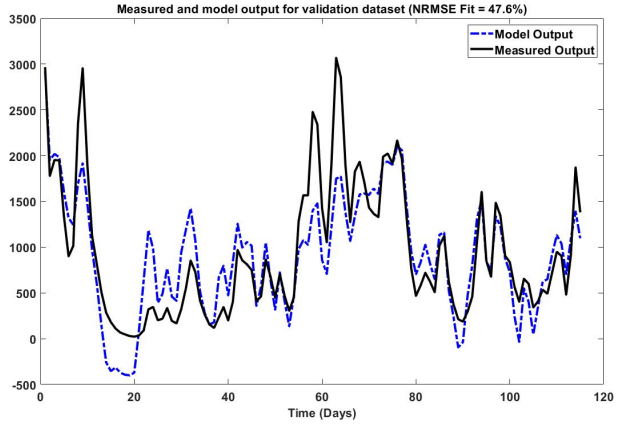

Fig. 4: Open-loop simulated output for validation dataset. The model generates NRMSE fits of 46.7% on validation and 57.2% on estimation dataset using a [2 [2 2 2] [1 1 1] ARX regressor structure.

1) Process Model: The MLD framework for a predictive model can be written as:

$$x_k = Ax_{k-1} + B_1u_{k-1} + B_2\delta_{k-1} + B_3z_{k-1} + B_dd_{k-1} \quad (10)$$

$$y_k = Cx_k + v_k \quad (11)$$

$$E_5 \geq E_2\delta_{k-1} + E_3z_{k-1} - E_4y_{k-1} - E_1u_{k-1} + E_dd_{k-1} \quad (12)$$

where $x_k \in \mathbb{R}^{n_x}$, $y_k \in \mathbb{R}^{n_y}$, $u_k \in \mathbb{R}^{n_u}$, and $d_k \in \mathbb{R}^{n_{dist}}$ represent state, output, manipulated variable, and measured disturbance vectors respectively. These comprise both continuous and categorical entries. The variables $\delta_k \in \{0,1\}^{n_d}$ and $z_k \in \mathcal{R}^{n_z}$ denote the binary and discrete categorical auxiliary variables and are implemented to translate the propositional logic into linear inequalities. Equation (12) encapsulates all propositional logic into its corresponding mixed integer linear inequality representation. The dimensions n_d and n_z are dependent on how the propositional logic is enforced on the system. $v_k \in \mathbb{R}^{n_y}$ is the lumped effects of unmeasured disturbances and noise in the outputs. It can be represented as:

$$\zeta_{k+1} = A_w\zeta_k + B_ww_k \quad (13)$$

$$v_k = C_w\zeta_k \quad (14)$$

where w_k denotes integrating white noise. The eigenvalues of A_w lie within a unit disk. v_k involves uncorrelated components associated with each output, resulting in $B_w = C_w = I$. $A_w = \text{diag}\{\Lambda_1, ;\cdots, ;\Lambda_{n_y}\}$, where $\Lambda_i = 0$ for Type-I disturbances and $\Lambda_i = 1$ for Type-II disturbances [6]. These equations allow the formulation of an extended state-space model [5] of the form:

$$\begin{aligned} X_{k+1} = \mathcal{A}X_k + \mathcal{B}_1\Delta u_k + \mathcal{B}_2\Delta\delta_k + \mathcal{B}_3\Delta z_k \\ + \mathcal{B}_d\Delta d_k + \mathcal{B}_w\Delta w_k \end{aligned} \quad (15)$$

$$y_k = \mathcal{C}X_k \quad (16)$$

C. Problem Formulation

The MPC cost for this hybrid system with slack variable ($\psi(k)$) is represented as follows:

$$\begin{aligned} J_k \triangleq \sum_{j=1}^{p}\|y_{k+j} - y_{r,k+j}\|^2_{W_y} + \sum_{i=0}^{m-1}\|\Delta u_{k+i}\|^2_{W_{du}} \\ + \sum_{i=0}^{m-1}\|u_{k+i} - u_{r,k+i}\|^2_{W_u} + \sum_{j=1}^{p}\|\psi_{k+j}\|^2_{W_s} \end{aligned} \quad (17)$$

where the minimization is performed over a prediction horizon p and move horizon m with respect to $u(k), \cdots, u(k+m-1), \delta(k), \cdots, \delta(k+p-1), z(k), \cdots, z(k+m-1), \psi(k), \cdots, \psi(k+p-1)$. The overall optimization problem can be denoted as:

$$\min_{u_{k+i},\ \delta_{k+j},\ z_{k+j},\ \psi_{k+j}} J_k \quad (18)$$

subject to constraints described in (12), (15)-(16), and

$$y_{\min} - \psi_{k+j} \leq y_{k+j} + \psi_{k+j} \leq y_{\max} \quad (19)$$

$$u_{\min} \leq u_{k+i} \leq u_{\max} \quad (20)$$

$$\Delta u_{\min} \leq \Delta u_{k+i} \leq \Delta u_{\max} \quad (21)$$

$$\psi_{k+j} \geq 0 \quad (22)$$

$$i = 0, 1, \cdots, m-1, \quad j = 1, 2, \cdots, p$$

Adding a slack variable facilitates optimization feasibility by relaxing constraints, crucial for hybrid problems where the precise optimum may be unattainable. Assigning a weight W_s keeps the solution within an acceptable range of optimality.

D. Three-Degree-of-Freedom Procedure

The HMPC formulation in this study employs a three-degree-of-freedom (3DoF) tuning [5], [10], enabling independent adjustment of setpoint tracking (α_r), measured disturbance rejection (α_d), and unmeasured disturbance rejection (f_y) based on desired closed-loop time constants. These parameters are computed as

$$\alpha_r = e^{-T_s/\tau_r}, \quad \alpha_d = e^{-T_s/\tau_d}, \quad f_y = 1 - e^{-T_s/\tau_u},$$

where T_s is the sampling time and τ_r, τ_d, τ_u are the corresponding time constants.

Setpoints and measured disturbances are filtered using Type-I/II digital filters [6] to regulate response speed. This study uses Type-I filters for both setpoint tracking and measured disturbance rejection, with tuning parameters α_r and α_d adjustable between 0 and 1, corresponding to desired response speeds τ_r and τ_d.

Unmeasured disturbance rejection is achieved through state observers, with corrections based on real-time output measurements. This involves a two-step method using Kalman filters with gain matrix $\mathcal{K}_f$ [5], allowing separate tuning for measured (α_d^j) and unmeasured disturbance (f_y) rejection speeds.

E. Logical Constraints for HMPC formulation

The $\beta(t)$ variable assumes values from a set of fixed levels defined as

$$\beta(t) \in L = \{\beta_1, \cdots, \beta_{n_\delta}\},$$

where n_δ denotes the number of discrete levels. This can be represented in the MLD format through the use of binary variables (δ_i) and auxiliary variables (z_i), where $i \in \{1, \cdots, n_\delta\}$. Among the set of binary variables $\delta_{i,k}$, only one is active at any given time instant k, corresponding to a lockdown level of $z_{i,k}$. The value of β_k at that moment is therefore determined by the active $z_{i,k}$, resulting in a quantized value. These associations are governed by the following relations:

$$\beta_k = \sum_{i=1}^{n_\delta} z_{i,k}\delta_{i,k}, \quad \sum_{i=1}^{n_\delta}\delta_{i,k} = 1, \quad (23)$$

$$\delta_{i,k} \in \{0,1\}, \quad \delta_{i,k} = 1 \iff z_{i,k} = L(i). \quad (24)$$

This set of constraints, along with (19)-(22), yield the set of E matrices in (12) needed for the estimation of the predictive model for the HMPC algorithm.

F. Formulation of HMPC for MLD Systems

Forecasting future output values y_k is essential to the HMPC algorithm for the MLD system. This can be achieved

by using the following sets of prediction equations involving filtered and unfiltered measured disturbances.

$$\mathcal{Y}_{flt,k+1} = \Phi X_{flt,k} + \mathcal{H}_1\mathcal{U}_k + \mathcal{H}_2\bar{\delta}_k + \mathcal{H}_3\mathcal{Z}_k + \mathcal{H}_d\mathcal{D}_{flt,k} - \mathcal{H}_{11}u_{k-1} - \mathcal{H}_{21}\delta_{k-1} - \mathcal{H}_{31}z_{k-1} - \mathcal{H}_{d1}d_{flt,k-1} \quad (25)$$

$$\mathcal{Y}_{k+1} = \Phi \hat{X}_k + \mathcal{H}_1\mathcal{U}_k + \mathcal{H}_2\bar{\delta}_k + \mathcal{H}_3\mathcal{Z}_k + \mathcal{H}_d\mathcal{D}_k - \mathcal{H}_{11}u_{k-1}\mathcal{H}_{21}\delta_{k-1} - \mathcal{H}_{31}z_{k-1} - \mathcal{H}_{d1}d_{k-1} \quad (26)$$

The variable and matrix definitions in (25)-(26) are detailed in [5]. Equation (25) applies a filtered output prediction to regulate the controller's reaction to setpoint and disturbance changes. In contrast, (26) ensures the unfiltered true output remains within system constraints. Similarly, (12) can be extended over the prediction horizon p as :

$$\mathcal{E}_5 \geq \mathcal{E}_2\bar{\delta}_k + \mathcal{E}_3\mathcal{Z}_k + \mathcal{E}_1\mathcal{U}_k + \mathcal{E}_d\mathcal{D}_k + \mathcal{E}_4\hat{X}_k - \mathcal{E}_{41}u_{k-1} - \mathcal{E}_{42}\delta_{k-1} - \mathcal{E}_{43}z_{k-1} - \mathcal{E}_{4d}d_{k-1} \quad (27)$$

where the matrices in (27) can be obtained from [5]. The solution to the optimization problem expressed in (18)-(22) can be obtained by control sequences that minimize (17). This can be done by utilizing (25) and (27) to formulate an MIQP of the form:

$$\min_{\xi_k} J_k \triangleq \frac{1}{2}\xi_k^T\mathcal{H}\xi_k + \mathcal{G}^T\xi_k \quad (28)$$

$$\tilde{\mathcal{S}}\xi_k \leq \mathcal{M} \quad (29)$$

where $\xi_k = [\mathcal{U}_k^T, \bar{\delta}_k^T, \mathcal{Z}_k^T, {\Psi_{k+1}}^T]^T$ denotes the vector of decision variables. The matrices utilized in (28) and (29) can be obtained from [5].

IV. Hybrid Control of SIR Infection using 3DoF-KFHMPC.

The HMPC framework illustrated in this paper restricts the movement of $\beta(t)$ to six levels: L = {10, 30, 50, 70, 100, 120} % of the initial level of contact among the population ($\overline{\beta}$); vaccination is continuous over a range.

A. Hybrid control - Standard case study

Figure 5 illustrates the ARX-based 3DoF-KF HMPC applied to the infection control problem by manipulating $\beta(t)$ and $k_v(t)$ under measured and unmeasured disturbances. The objective is a 90% reduction in the infected population at $t = 5$ days, with a setpoint of 50% on $\beta(t)$ and an upper limit of 50% on $k_v(t)$ throughout the study. The system experiences a measured disturbance from recovery ($\Delta\gamma = 0.4$ Day^{-1}) at $t = 70$ days and an unmeasured disturbance from loss of immunity ($\Delta\rho = 0.4$ Day^{-1}) at $t = 100$ days. Controller parameters are detailed in Table II. The controller rapidly adjusts lockdown and vaccination to achieve a 90% infection reduction while adhering to system constraints, as shown in Figure 5. Upon the measured recovery disturbance at $t = 70$ days, the controller promptly relaxes vaccination requirements until the loss of immunity at $t = 100$ days.

TABLE II: Control design parameters for the *SIR* problem

Parameter	Value	Parameter	Value
p	50 Days	y_{min}	0
m	20 Days	y_{max}	∞
τ_r	1 Day	Δu_{min}	$[-0.5\overline{\beta}$ -$\infty]$
τ_d	0.5 Day	Δu_{max}	[∞ 0.1 Day^{-1}]
τ_u	0.5 Day	W_y	1
u_{min}	[0.07$\overline{\beta}$ 0]	W_{du}	[0.1 0.01]
u_{max}	[∞ 0.5 Day^{-1}]	W_{slack}	1e-7
W_u	[1 0]	β_{target}	0.5 $\overline{\beta}$

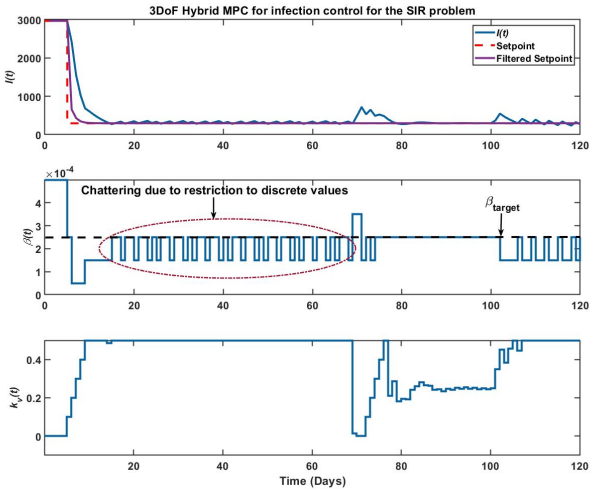

Fig. 5: 3DoF HMPC for the SIR problem. Setpoint change of 90% reduction in I at t = 5 days. Measured disturbance ($\Delta\gamma$ = 0.4 Day^{-1}) at t = 70 days. Unmeasured disturbance ($\Delta\rho$ = 0.4 Day^{-1}) at t = 100 days. The manipulated variable takes only categorical values, resulting in chattering..

Although the control actions effectively reduce the infected population under both measured and unmeasured disturbances, a key limitation is the noticeable chattering in the closed-loop system. As a result of the categorical nature of the lockdown policy, $\beta(t)$ alone cannot achieve the exact value needed for zero offset while maintaining a fixed setpoint when the $k_v(t)$ reaches its upper constraint, causing consecutive corrective actions for overshoots and undershoots throughout the study. Chattering worsens with a target for $\beta(t)$ set at 50% of its initial steady-state value $\overline{\beta}$. The conflicting setpoints on $I(t)$ and $\beta(t)$ force the manipulated variables to move in opposite directions as vaccination reaches its upper saturation limit of 50%, further amplifying $\beta(t)$ oscillations. In reality, this results in frequent switching between lockdown states, creating confusion.

However, vaccination provides a smoother response. Unlike lockdown, which is restricted to discrete levels, vaccination rates can be incrementally adjusted based on outbreak severity, showcasing the advantage of the MIMO formulation. Lockdown alone proves inefficient due to large discrete jumps, whereas combining vaccination with lockdown offers a more sustainable, long-term solution, reducing reliance on disruptive distancing interventions as the population grows increasingly immune to the infection.

B. Hybrid control - With reconfiguration policy

To mitigate chattering in the standard case study, a reconfiguration policy is introduced into the closed-loop system, as shown in Figure 6. This flexible formulation allows the controller to temporarily relax output setpoint tracking once the infection $I(t)$ falls within a specified band around the desired value. This is attained by setting W_y = 0 as $I(t)$

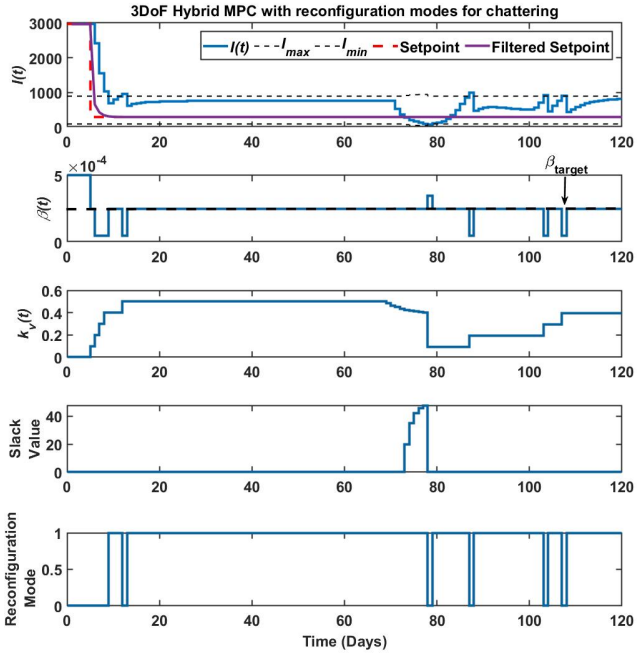

Fig. 6: The HMPC with reconfiguration maintains infection levels within the acceptable bounds [100, 900], though slightly above the true setpoint. The slack weight on bounds is $W_s = 1\text{e}^{-07}$. The manipulated variable shows no chattering. The reconfiguration indicator marks periods within the reconfiguration zone as 1, while violations from nonlinearity or disturbances are marked as 0.

reaches the pre-defined acceptable region. The slack Ψ_k, move size constraints $[\Delta u_{min} \quad \Delta u_{max}]$, and the weight on the lockdown setpoint W_u, however, continue to remain active. A new set of constraints is imposed on the infection during reconfiguration that ensures it stays within the desired region with minimal control actions in terms of lockdown. Factors such as system nonlinearity, or measured and unmeasured disturbances may throw the infection out of the reconfiguration zone (see Reconfiguration Indicator; Figure 6, Subplot 4, 0 denotes normal operation, while 1 denotes the reconfiguration mode), which would reimpose the weights on the setpoint tracking, thereby ensuring limited deviation from the desired value of the infected population while eliminating the chattering in the input or the output of the system. The initial oscillation in $\beta(t)$ can be explained through the presence of the $0.5\overline{\beta}$ setpoint on the lockdown.

Given the availability of vaccination $k_v(t)$ as a manipulated variable, the controller is able to increase $\beta(t)$ to its desired target once the weight on $I(t)$ is removed upon entering the reconfiguration region, where it remains constant up until the measured disturbance in $\gamma(t)$ is encountered. This, therefore, presents a significantly more practical implementation of the control action with judicious use of lockdown and in the context of infectious disease prevention. A downside of this approach is that, although within an acceptable level, the infected population remains higher than in a scenario where strict setpoint tracking is mandated through non-zero output tracking weight. In such a scenario, the system would be more prone to disturbances pushing the infection outside the reconfiguration region, resulting in a resumption of aggressive control actions and potentially longer periods of infection. Therefore, this approach can be incorporated in a situation where a tradeoff can be accepted between socially sustainable lockdown policies and higher levels of infection.

V. Conclusions and Future Work

Data-driven modeling and control have gained popularity in addressing complex dynamic systems. The COVID-19 pandemic has renewed interest in control systems for managing public health interventions. This paper proposes a robust strategy for managing infection trajectories by integrating a MIMO 3DoF-KF HMPC framework with a data-driven ARX model. Systematic experiment design and ARX modeling capture infection dynamics with minimal engineering effort, while the 3DoF-KF formulation provides intuitive and flexible real-world policymaking for epidemiological applications. The hybrid approach ensures physically realizable control actions for disease-spread scenarios. Future work will explore integrating Model-on-Demand (MoD) [10] with MIMO 3DoF-KF HMPC. Initial efforts improved open-loop performance (Section III-A) but offered limited closed-loop improvements. However, MoD's benefits go beyond its closed-loop performance, owing to the insights attained through the study of adaptively changing models, potentially generating more informed epidemic management policies.

Acknowledgment

This research work has been supported by the National Science Foundation (US) through the Predictive Intelligence for Pandemic Preparedness (PIPP) program grant 2200161. The opinions in this paper are the authors' own and do not necessarily reflect the views of the NSF.

References

[1] W. O. Kermack and A. G. McKendrick, "A contribution to the mathematical theory of epidemics," *Proceedings of the Royal Society of London. Series A, Containing Papers of a Mathematical and Physical Character*, vol. 115, no. 772, pp. 700–721, 1927.

[2] C. M. Simon, "The SIR dynamic model of infectious disease transmission and its analogy with chemical kinetics," *PeerJ Physical Chemistry*, vol. 2, p. e14, 2020.

[3] D. E. Rivera, S. Banerjee, C. Kobs, M. El Mistiri, and Z. Shi, "SIR Epidemic Control Using a 2DoF IMC-PID with Filter Control Strategy," *IFAC-PapersOnLine*, vol. 58, no. 7, pp. 204–209, 2024.

[4] J. Köhler, L. Schwenkel, A. Koch, J. Berberich, P. Pauli, and F. Allgöwer, "Robust and optimal predictive control of the COVID-19 outbreak," *Annual Reviews in Control*, vol. 51, pp. 525–539, 2021.

[5] O. Khan, M. El Mistiri, S. Banerjee, E. Hikler, and D. E. Rivera, "3DoF-KF HMPC: A Kalman filter-based Hybrid Model Predictive Control Algorithm for Mixed Logical Dynamical Systems," *Control Engineering Practice*, vol. 154, p. 106171, 2025.

[6] M. Morari and E. Zafiriou, *Robust Process Control*. Englewood Cliffs, NJ: Prentice-Hall, 1989.

[7] L. Ljung, *System Identification: Theory for the User*, 2nd ed. Upper Saddle River, NJ: Prentice Hall PTR, 1999.

[8] P. Guillaume, J. Schoukens, R. Pintelon, and I. Kollar, "Crest-factor minimization using nonlinear Chebyshev approximation methods," *IEEE Trans. Instrum. Meas.*, vol. 40, no. 6, pp. 982–989, 1991.

[9] D. E. Rivera, H. Lee, H. D. Mittelmann, and M. W. Braun, "Constrained multisine input signals for plant-friendly identification of chemical process systems," *Journal of Process Control*, vol. 19, no. 4, pp. 623–635, 2009.

[10] S. Banerjee, O. Khan, M. El Mistiri, N. N. Nandola, and D. E. Rivera, "Data-Driven Control of Highly Interactive Systems using 3DoF Model-On-Demand MPC: Application to a MIMO CSTR," *IFAC-PapersOnLine*, vol. 58, no. 15, pp. 420–425, 2024.